Polyhedron 27 (2008) 2771–2778

Contents lists available at ScienceDirect

Polyhedron

journal homepage: www.elsevier.com/locate/poly

Synthesis, structure, and electrochemistry of pyridinecarboxamide cobalt(III) complexes; the effect of bridge substituents on the redox properties

Soraia Meghdadi [a], Mehdi Amirnasr [a,*], Mohammad H. Habibi [b], Ahmad Amiri [a], Vahid Ghodsi [a], Azadeh Rohani [a], Ross W. Harrington [c], William Clegg [c]

[a] Department of Chemistry, Isfahan University of Technology, Isfahan 84156-83111, Iran
[b] Department of Chemistry, University of Isfahan, Isfahan 81746-73441, Iran
[c] School of Chemistry, Newcastle University, Newcastle upon Tyne NE1 7RU, UK

ARTICLE INFO

Article history:
Received 27 March 2008
Accepted 26 May 2008
Available online 18 July 2008

Keywords:
Bispyridylamide complexes of Co(III)
Substituted N_4-amido ligand
Crystal structure
Cyclic voltammetry

ABSTRACT

Two series of complexes of the types *trans*-[Co^{III}(Mebpb)(amine)$_2$]ClO_4 {Mebpb^{2-} = *N*,*N*-bis(pyridine-2-carboxamido)-4-methylbenzene dianion, and amine = pyrrolidine (prldn) (**1a**), piperidine (pprdn) (**2a**), morpholine (mrpln) (**3a**), benzylamine (bzlan) (**4a**)}, and *trans*-[Co^{III}(cbpb)(amine)$_2$]X {cbpb^{2-} = *N*,*N*-bis(pyridine-2-carboxamido)-4-chlorobenzene dianion, and amine = pyrrolidine (prldn), X = PF_6 (**1b**), piperidine (pprdn), X = PF_6 (**2b**), morpholine (mrpln), X = ClO_4 (**3b**), benzylamine (bzlan), X = PF_6 (**4b**)} have been synthesized and characterized by elemental analyses, IR, UV–Vis, and ^{1}H NMR spectroscopy. The crystal structure of **1a** has been determined by X-ray diffraction. The electrochemical behavior of these complexes, with the goal of evaluating the effect of axial ligation and equatorial substitution on the redox properties, is also reported. The reduction potential of Co^{III}, ranging from −0.53 V for (**1a**) to −0.31 V for (**3a**) and from −0.48 V for (**1b**) to −0.22 V for (**3b**) show a relatively good correlation with the σ-donor ability of the axial ligands. The methyl and chloro substituents of the equatorial ligand have a considerable effect on the redox potentials of the central cobalt ion and the ligand-centered redox processes.

1. Introduction

The binding of metal ions by proteins and peptides is of fundamental interest due to the importance of metal ions in biological systems [1]. The carboxamide [–C(O)NH–] group, ubiquitous throughout nature in the primary structure of proteins, is an important ligand construction unit for coordination chemists. Pyridinecarboxamides, a burgeoning class of multidentate ligands containing this linkage, are available from condensation reactions between pyridyl-bearing amine or carboxylic acid precursors, promoted by coupling agents such as 1,1′-carbonyldiimadazole, diphenylphosphoryl azide or triphenylphosphite [2–6]. These ligands have found use in asymmetric catalysis [3,7], molecular receptors and dendrimer synthesis [8–10], and platinum(II) complexes with antitumor properties [5]. Transition metal complexes of dianionic bis(amide) ligands, derived from picolinic acid and 2,6-pyridinedicarboxylic acid, are subject to electrochemical oxidation at both metal and ligand sites to form metal- and ligand-centered oxidation products, respectively [6,11–16].

Complexes of somewhat similar ligands containing two pyridine-2-carboxamide groups have been extensively studied in recent years [17–31]. The deprotonated amide is a strong σ-donor capable of stabilizing early as well as late metal ions in high oxidation states [21–23], making high-valent metal complexes of the ligands suitable as Lewis acid catalysts. Although a large number of metal complexes have been characterized and their electrochemical, spectroscopic and magnetic properties as well as their ligand exchange ability studied, it is only recently that they have found more extensive applications in catalysis [27,28]. One factor which makes the ligands attractive for catalytic applications is the simplicity whereby the structure of the ligands can be modified by a modular approach. The electronic and steric properties can conveniently be modified by altering the diamine backbone and by the introduction of suitable substituents in the pyridine nuclei [12]. Since the pyridine nitrogen atom resembles imidazole nitrogen, metal complexes of bispyridylamides have also been employed as models for metalloenzymes [27].

As part of our continued interest in the transition-metal chemistry of dianionic bispyridylamide ligands [25,30,31], herein we describe the synthesis and spectroscopic characterization of a group of diaxially ligated octahedral complexes of Co^{III} with Mebpb^{2-} and cbpb^{2-} as equatorial ligands (Scheme 1). The crystal structure

---

* Corresponding author. Tel.: +98 311 391 2351; fax: +98 311 391 2350.
E-mail address: amirnasr@cc.iut.ac.ir (M. Amirnasr).

0277-5387/$ - see front matter © 2008 Elsevier Ltd. All rights reserved.
doi:10.1016/j.poly.2008.05.031

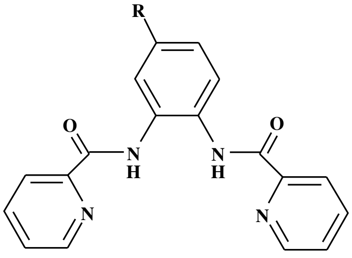

R	Ligand
CH_3	H_2Mebpb
Cl	H_2cbpb

Scheme 1.

of a representative complex, *trans*-[Co(Mebpb)(prldn)$_2$]ClO$_4$, has been determined. The IR, UV–Vis, and ^{1}H NMR spectra of the complexes are also reported and discussed. The electrochemical behavior of the complexes has also been investigated with the goal of evaluating the effects of axial ligation and equatorial substitution on their redox properties.

2. Experimental

2.1. Materials and general methods

All solvents and chemicals were of commercial reagent grade and used as received from Aldrich and Merck. Elemental analyses were performed by using a Perkin–Elmer 2400II CHNS-O elemental analyzer. UV–Vis spectra were recorded on a Jasco V-570 spectrophotometer. Infrared spectra (KBr pellets) were obtained on a Jasco 680-plus FT-IR spectrophotometer. The ^{1}H NMR spectra of the complexes were obtained on a Bruker AVANCE DR X500 (500 MHz) spectrometer. Proton chemical shifts are reported in parts per million (ppm) relative to an internal standard of Me$_4$Si. Cyclic voltammograms were recorded by using a Sama Research Analyzer M-500. Three electrodes were utilized in this system, a glassy carbon working electrode, a platinum disk auxiliary electrode, and Ag wire as reference electrode. The glassy carbon working electrode (Metrohm 6.1204.110) with 2.0 ± 0.1 mm diameter was manually cleaned with 1 μm alumina polish prior to each scan. Tetrabutylammonium hexafluorophosphate (TBAH) was used as supporting electrolyte. Acetonitrile was dried over CaH$_2$. The solutions were deoxygenated by purging with Ar for 5 min. All electrochemical potentials were calibrated versus internal Fc$^{+/0}$ (E^0 = 0.40 V versus SCE) couple under the same conditions [32].

Caution: Perchlorate salts with organic compounds are potentially explosive and should be handled with care.

2.2. Synthesis

2.2.1. H_2Mebpb

4-Methyl-1,2-phenylenediamine was recrystallized from hot ligroin before use. The ligand was prepared according to the method described in the literature with some modification [18]. To a solution of 2-pyridinecarboxylic acid (7.38 g, 60 mmol) in pyridine (25 mL) in a two-necked round-bottom flask equipped with mechanical stirrer was added a solution of 4-methyl-1,2-phenylenediamine (3.66 g, 30 mmol) in 5 mL pyridine, and the mixture stirred at 40 °C for 40 min. Triphenylphosphite (15.6 mL, 60 mmol) was then added dropwise and the reaction mixture was stirred at 90–100 °C for 4 h. Upon cooling to room temperature the product precipitated as a microcrystalline solid. The resulting precipitate was filtered off, washed with ethanol (20 mL), and recrystallized from a mixture of methanol and water (2:1 v/v). Yield (70%). m.p. 168–169 °C. FT-IR (KBr, cm^{-1}) ν_{max}: 3302 (s, N–H), 1689, 1659 (s, C=O), 1589 (m, C=C), 1520 (m, C–N). UV–Vis: λ_{max} (nm) (ε, L M^{-1} cm^{-1}) (CH$_3$CN): 300 (9427), 267 (15 662), 219 (26 563).

2.2.2. H_2cbpb

H_2cbpb was synthesized by a procedure similar to that for H_2Mebpb, but 4-chloro-1,2-phenylenediamine was used instead of 4-methyl-1,2-phenylenediamine. The product was recrystallized from ethanol. Yield (70%). m.p. 196–198 °C. *Anal.* Calc. for $C_{18}H_{13}N_4O_2Cl$: C, 61.28; H, 3.71; N, 15.88. Found: C, 61.28; H, 3.61; N, 15.81%. FT-IR (KBr, cm^{-1}) ν_{max}: 3297 (s, N–H), 1697, 1661 (s, C=O), 1588 (m, C=C), 1506 (s, C–N). UV–Vis: λ_{max} (nm) (ε, L M^{-1} cm^{-1}) (CH$_3$CN): 300 (10 735), 267 (18 627), 211 (35 942). ^{1}H NMR (CDCl$_3$, 300 MHz): δ = 10.32, 10.19 (2H, NH$_{amidic}$, s), 8.56 (2H$_a$, dd, J = 9.8, 4.4), 8.31 (2H$_d$, d, J = 7.8), 8.03 (1H$_g$, d, J = 7.8), 7.92 (2H$_c$, dd, J = 7.7, 7.7), 7.81 (1H$_e$, d, J = 8.6), 7.48 (2H$_b$, m), 7.26 (1H$_f$, d, J = 8.0).

2.2.3. Synthesis of trans-[Co(Mebpb)(prldn)$_2$] ClO$_4$ (**1a**)

To a solution of Co(CH$_3$COO)$_2$ · 4H$_2$O (62.3 mg, 0.25 mmol) in methanol (20 mL) was added a boiling solution of H_2Mebpb (83.1 mg, 0.25 mmol) in methanol (30 mL). To this solution was added dropwise 9.07 mmol (0.75 mL) of pyrrolidine and air was bubbled through the reaction mixture for 3 h. The final reaction mixture was filtered, a solution of 0.25 mmol (30.6 mg) of NaClO$_4$ · H$_2$O in methanol was slowly added to the filtrate, and the resulting solution was stirred for 5 min. Dark blue crystals were obtained by slow evaporation of methanol. The crystals were isolated by filtration, washed with methanol, and dried in vacuum. Yield: 75%. *Anal.* Calc. for $C_{27}H_{32}N_6O_6ClCo$: C, 51.4; H, 5.11; N, 13.32. Found: C, 50.73; H, 5.29; N, 13.11%. FT-IR (KBr, cm^{-1}) ν_{max}: 3168 (s, N–H), 1626 (s, C=O), 1599 (s, C=C), 1571 (s, C–N), 1109, 1087 (s, Cl–O). UV–Vis: λ_{max} (nm) (ε, L M^{-1} cm^{-1}) (CH$_3$CN): 625 (180), 418 (6686). ^{1}H NMR (CD$_3$CN, 500 MHz): δ = 1.29 (8H$_i$, m), 1.55, 2.12 (8H$_h$, m), 2.39 (3H, CH$_3$, s), 3.30 (2H, amine NH, br s), 6.94 (1H$_f$, d, J = 8.2), 8.00–8.39 (6H $_{b,c,d}$, m), 8.71 (1H$_g$, s), 8.75 (1H$_e$, d, J = 8.2), 9.46 (2H$_a$, dd, 5.2, 5.2).

2.2.4. Synthesis of trans-[Co(cbpb)(prldn)$_2$] PF$_6$ (**1b**)

To a solution of Co(CH$_3$COO)$_2$ · 4H$_2$O (62.3 mg, 0.25 mmol) in methanol–ethanol (2:1 v/v) (20 mL) was added a boiling solution of H_2cbpb (88.2 mg, 0.25 mmol) in methanol–ethanol (2:1 v/v) (30 mL). To this solution was added dropwise 9.07 mmol (0.75 mL) of pyrrolidine and air was bubbled through the reaction mixture for 3 h. The volume of the reaction mixture was increased to 75 mL by adding methanol and the final solution was filtered. A solution of 0.25 mmol (40.6 mg) of ammonium hexafluorophosphate in methanol–ethanol (2:1v/v) (25 mL) was slowly added to the filtrate and the resulting solution stirred for 5 min. Green-blue crystals were obtained by slow evaporation of solvent. The crystals were isolated by filtration, washed with cold methanol, and dried in vacuum. Yield: 75%. *Anal.* Calc. for $C_{29}H_{29}N_6O_2ClPF_6Co$: C, 44.81; H, 4.19; N, 12.05. Found: C, 44.54; H, 4.09; N, 11.91%. FT-IR (KBr, cm^{-1}) ν_{max}: 3171 (s, N–H), 1629 (s, C=O), 1600 (s, C=C), 1563 (s, C–N), 842 (s, PF$_6$). UV–Vis: λ_{max} (nm) (ε, L M^{-1} cm^{-1}) (CH$_3$CN): 611 (188), 410 (7354). ^{1}H NMR (CD$_3$CN, 500 MHz): δ = 1.30 (8H$_i$, m), 1.52, 2.12 (8H$_h$, m), 3.28 (2H, NH$_{amine}$, br s), 7.11 (1H$_f$, bd, J = 8.6), 7.99–8.41 (6H$_{b,c,d}$, m), 8.82–8.83 (2H, H$_e$, H$_g$), 9.42 (2H$_a$, bd, J = 4.8).

2.2.5. Synthesis of trans-[Co(Mebpb)(pprdn)$_2$]ClO$_4$ (**2a**)

To a solution of Co(CH$_3$COO)$_2$ · 4H$_2$O (62.3 mg, 0.25 mmol) in 20 mL ethanol–methanol (1:2 v/v) was added a boiling solution of H_2Mebpb (83.1 mg, 0.25 mmol) 30 mL ethanol–methanol (1:2

v/v). To this solution was added dropwise 7.58 mmol (0.75 mL) of piperidine and air was bubbled through the reaction mixture for 3 h. The final reaction mixture was filtered and a solution of 0.25 mmol (30.6 mg) of $NaClO_4 \cdot H_2O$ in methanol was added slowly to the filtrate. Dark green-blue crystals were obtained by slow evaporation of solvent. The crystals were isolated by filtration, washed with a mixture of ethanol and methanol (1:2 v/v), and dried in vacuum. Yield: 80%. *Anal.* Calc. for $C_{29}H_{36}N_6O_6ClCo$: C, 52.85; H, 5.51; N, 12.75. Found: C, 52.32; H, 6.1; N, 12.2%. FT-IR (KBr, cm^{-1}) ν_{max}: 3162 (s, N–H), 1626 (s, C=O), 1599 (s, C=C), 1565 (s, C–N), 1111, 1087 (s, Cl–O). UV–Vis: λ_{max} (nm) (ε, $L\,M^{-1}\,cm^{-1}$) (CH_3CN): 682 (193), 417 (6532). ^1H NMR (CD_3CN, 500 MHz): δ = 0.91–1.28 ($12H_{i,j}$, m), 1.40–2.22 ($8H_h$, m), 2.39 (3H, CH_3, s), 2.45 (2H, NH_{amine}, br s), 6.93 ($1H_f$, d, J = 7.9), 8.00–8.41 ($6H_{b,c,d}$, m), 8.71 (H_g, s), 8.75 (H_e, d, 8.2) 9.39 ($2H_a$, br d, J = 5.0).

2.2.6. Synthesis of trans-[Co(cbpb)(pprdn)$_2$]PF$_6$ (**2b**)

This complex was prepared by the same method as for **1b** except that piperidine was used instead of pyrrolidine. Dark green-blue crystals were obtained after 5 days; they were filtered off, washed with a small amount of cold methanol, and dried in vacuum. Yield: 65%. *Anal.* Calc. for $C_{28}H_{33}N_6O_2ClPF_6Co$: C, 46.39; H, 4.58; N, 11.59. Found: C, 45.52; H, 4.52; N, 11.25%. FT-IR (KBr, cm^{-1}) ν_{max}: 3173 (s, N–H), 1627 (s, C=O), 1600 (s, C=C), 1562 (s, C–N), 841 (s, PF_6). UV–Vis: λ_{max} (nm) (ε, $L\,M^{-1}\,cm^{-1}$) (CH_3CN): 656 (205), 409 (7434). ^1H NMR (CD_3CN, 500 MHz): δ = 0.9–1.29 ($12H_{i,j}$, m), 1.35–2.22 ($8H_h$, m), 2.47 (2H, NH_{amine}, br s), 7.12 ($1H_f$, d, J = 8.6), 7.95–8.45 ($6H_{b,c,d}$, m), 8.83–8.87 (2H, H_e, H_g), 9.36 ($2H_a$, br d, J = 4.8).

2.2.7. Synthesis of trans-[Co(Mebpb)(mrpln)$_2$] ClO$_4$ (**3a**)

To a solution of $Co(CH_3COO)_2 \cdot 4H_2O$ (62.3 mg, 0.25 mmol) in methanol (5 mL) was added a solution of H_2Mebpb (83.1 mg, 0.25 mmol) in acetone (50 mL). To this solution was added dropwise morpholine (8.61 mmol, 0.75 mL) and air was bubbled through the reaction mixture for 3 h. The final reaction mixture was filtered and a solution of 0.25 mmol (30.6 mg) of $NaClO_4 \cdot H_2O$ in acetone was added slowly to the filtrate. Dark green-blue crystals were isolated by filtration, washed with a mixture of acetone and methanol (1:9 v/v), and dried in vacuum. Yield: 70%. *Anal.* Calc. for $C_{27}H_{32}N_6O_8ClCo$: C, 48.92; H, 4.86; N, 12.68. Found: C, 48.01; H, 5.18; N, 12.64%. FT-IR (KBr, cm^{-1}) ν_{max}: 3141 (m, N–H), 1626 (s, C=O), 1599 (s, C=C), 1566 (m, C–N), 1111, 1091 (s, Cl–O). UV–Vis: λ_{max} (nm) (ε, $L\,M^{-1}\,cm^{-1}$) (CH_3CN): 689 (198), 412 (8134). ^1H NMR (CD_3CN, 500 MHz): δ = 1.65–1.95 ($8H_h$, overlaps with solvent signals), 2.39 (3H, CH_3, s), 2.97 (2H, NH_{amine}, br s), 3.20 ($8H_i$, m), 6.95 ($1H_f$, d, J = 7.9), 8.02–8.44 ($6H_{b,c,d}$, m), 8.73 ($1H_g$, s), 8.75 ($1H_e$, d, J = 8.2), 9.42 ($2H_a$, br d, J = 4.9).

2.2.8. Synthesis of trans-[Co(cbpb)(mrpln)$_2$] ClO$_4$ (**3b**)

To a solution of $Co(CH_3COO)_2 \cdot 4H_2O$ (24.9 mg, 0.1 mmol) in methanol–ethanol (2:1 v/v) (20 mL) was added a solution of H_2cbpb (35.3 mg, 0.1 mmol) in methanol–ethanol (2:1 v/v) (30 mL). To this solution was added dropwise morpholine (8.61 mmol, 0.75 mL) and air was bubbled through the reaction mixture for 3 h. The volume of the reaction mixture was increased to 75 mL by adding methanol and the final solution was filtered. A solution of 0.1 mmol (12.2 mg) of $NaClO_4 \cdot H_2O$ in methanol–ethanol (2:1 v/v) (25 mL) was slowly added to the filtrate and the resulting solution stirred for 5 min. Green-blue crystals were obtained by slow evaporation of solvent. The crystals were isolated by filtration, washed with mixture of diethyl ether and methanol (1:9 v/v) and dried in vacuum. Yield: 65%. *Anal.* Calc. for $C_{26}H_{29}N_6O_8Cl_2Co$: C, 45.69; H, 4.28; N, 12.29. Found: C, 45.35; H, 4.29; N, 12.00%. FT-IR (KBr, cm^{-1}) ν_{max}: 3169 (m, N–H), 1626 (s, C=O), 1600 (s, C=C), 1562 (s, C–N), 1119, 1089 (s, ClO_4). UV–Vis: λ_{max} (nm) (ε, $L\,M^{-1}\,cm^{-1}$) (CH_3CN): 663 (232), 405 (7061). ^1H NMR (CD_3CN, 500 MHz): δ = 1.61, 2.98 ($8H_h$, m), 3.55 (2H, NH_{amine}, br s), 3.21 ($8H_i$, m), 7.09 ($1H_f$, m), 7.81–8.48 ($6H_{b,c,d}$, m), 8.82–8.91 ($2H_{e,g}$, m), 9.39 ($2H_a$, br d, J = 4.8).

2.2.9. Synthesis of trans-[Co(Mebpb)(bzlan)$_2$] ClO$_4$ (**4a**)

To a solution of $Co(CH_3COO)_2 \cdot 4H_2O$ (24.9 mg, 0.1 mmol) in methanol (20 mL) was added a boiling solution of H_2 Mebpb (33.2 mg, 0.1 mmol) in methanol (30 mL). To this solution was added dropwise 6.86 mmol (0.75 mL) benzylamine and air was bubbled through the reaction mixture for 3 h. The final reaction mixture was filtered and a solution of 0.1 mmol (12.2 mg) of $NaClO_4 \cdot H_2O$ in methanol was added slowly to the filtrate. Dark green-blue crystals were isolated by filtration, washed with a mixture of ethanol and diethyl ether (9:1 v/v), and dried in vacuum. Yield: 65%. *Anal.* Calc. for $C_{33}H_{32}N_6O_6ClCo$: C, 56.38; H, 4.59; N, 11.95. Found: C, 56.10; H, 4.52; N, 11.84%. FT-IR (KBr, cm^{-1}) ν_{max}: 3251, 3214, 3135 (m, m, s, N–H), 1628 (s, C=O), 1601 (s, C=C), 1566 (s, C–N), 1094, 1081 (s, Cl–O). UV–Vis: λ_{max} (nm) (ε, $L\,M^{-1}\,cm^{-1}$) (CH_3CN): 610 (235), 414 (7013). ^1H NMR (CD_3CN, 500 MHz): δ = 2.42 (3H, CH_3, s), 2.74 ($4H_h$, m), 2.91 (4H, NH_{2amine}, br s), 6.74 ($4H_i$, bd), 7.09–7.15 ($6H_{j,k}$, m), 6.96($1H_f$,d, J = 8.2), 7.94–8.35 ($6H_{b,c,d}$, m), 8.75 ($1H_g$, s), 8.78 ($1H_e$, d, J = 8.2), 9.41 ($2H_a$, dd, J = 4.6, 4.6, 4.6).

2.2.10. Synthesis of trans-[Co(cbpb)(bzlan)$_2$] PF$_6$ (**4b**)

This complex was prepared by the same method as for **1b** except that benzylamine was used instead of pyrrolidine. Dark green-blue crystals were obtained after one week; they were filtered off, washed with a mixture of ethanol and diethyl ether (9:1 v/v), and dried in vacuum. Yield: 65%. *Anal.* Calc. for $C_{32}H_{29}N_6O_2ClPF_6Co$: C, 49.98; H, 3.80; N, 10.93. Found: C, 49.11; H, 3.80; N, 10.66%. FT-IR (KBr, cm^{-1}) ν_{max}: 3213, 3133 (m, N–H), 1629 (s, C=O), 1601 (s, C=C), 1562 (s, C–N), 843 (s, PF_6). UV–Vis: λ_{max} (nm) (ε, $L\,M^{-1}\,cm^{-1}$) (CH_3CN): 607 (224), 408 (7210). ^1H NMR (CD_3CN, 500 MHz): δ = 2.74 ($4H_h$, m), 3.05 (4H, NH_{2amine}, br s), 6.75 ($4H_i$, bd, 7.6), 7.05–7.16 ($7H_{j,k,f}$, m), 7.96–8.33 ($6H_{b,c,d}$, m), 8.73–8.76 ($2H_{e,g}$, m), 9.41 ($2H_a$, br d).

2.3. X-ray crystallography

Dark blue crystals of **1a** suitable for X-ray crystallography were obtained from methanol. Data were collected at 150 K, on a Nonius KappaCCD diffractometer (Mo Kα radiation, λ = 0.71069 Å) using

Table 1
Crystal data and structure refinement for (**1a**)

Chemical formula	$[C_{27}H_{32}CoN_6O_2]^{+}ClO_4^{-}$
Formula weight	631.0
Crystal system	triclinic
Space group	$P\bar{1}$
a (Å)	9.382(5)
b (Å)	11.788(5)
c (Å)	13.361(5)
α (°)	84.155(5)
β (°)	81.886(5)
γ (°)	82.339(5)
V (Å^3)	1444.6(11)
Z, D_{Calc} (g cm^{-3})	2, 1.451
Crystal size (mm)	0.40 × 0.40 × 0.35
μ (mm^{-1})	0.738
Reflections collected	29046
Independent reflections (R_{int})	5671 (0.0293)
Transmission factors	0.757–0.782
Refined parameters	381
Goodness-of-fit on F^2	1.108
R ($F^2 > 2\sigma$)	0.0680
R_w (F^2, all data)	0.2070
Maximum and minimum electron density (e Å^{-3})	1.89 and −1.22

the COLLECT [33] program. Cell refinement and data reduction were performed with EVALCCD [34]. Crystal data, together with other relevant information on structure determination, are listed in Table 1. An empirical absorption correction, based on repeated and equivalent reflections, was carried out using SADABS [35]. The structure was solved by SIR97 [36] and refined, against F^2, by SHELXTL [37]. Anisotropic displacement parameters were assigned to all the non-hydrogen atoms. Hydrogen atoms were placed in idealized positions and allowed to ride on their respective parent atoms. The major residual electron density features are close to the anion, which is probably subject to unresolved disorder.

3. Results and discussion

3.1. Synthesis

All complexes were prepared by the following general method. To a solution of $Co(CH_3COO)_2 \cdot 4H_2O$ in an appropriate solvent was added an equimolar amount of ligand in an appropriate solvent. A vigorous stream of air was passed through this solution, to which was gradually added excess amine. The air oxidation was continued for a period of 3 h, during which the color changed from red-brown to green-blue. Dark green-blue crystals of these complexes were obtained in good yield (65–80%).

3.2. Description of structure of trans-[Co(Mebpb)(prldn)$_2$]ClO$_4$ (**1a**)

To the best our knowledge, this is only the second reported structure of a $[Co^{III}(bpb)(amine)_2]^+$ complex containing neutral *N*-donor axial ligands. Fig. 1 shows the molecular structure of **1a** with the atomic numbering scheme. The structure exhibits a distorted octahedral environment around cobalt. Selected bond angles and distances are listed in Table 2. As expected, the ligand ($Mebpb^{2-}$) in **1a** binds to the trivalent metal ion (Co^{III}) via two pyridine N atoms and two amido N atoms in the equatorial plane of the octahedron. There are two pyrrolidine molecules attached to the metal to fill its axial sites. All Co–N bond distances are within the range 1.892(3)–2.012(3) Å, and are indicative of a low-spin $(t_{2g})^6$ configuration of the central Co^{III} ion [22].

Table 2
Selected bond lengths (Å) and angles (°) for (**1a**)

Bond lengths	
Co–N1	1.997(3)
Co–N2	1.892(3)
Co–N3	1.892(3)
Co–N4	1.994(3)
Co–N5	1.992(3)
Co–N6	2.012(3)
Bond angles	
N1–Co–N2	82.88(13)
N1–Co–N3	166.85(14)
N1–Co–N4	110.63(13)
N1–Co–N5	90.16(13)
N1–Co–N6	89.36(13)
N2–Co–N3	84.10(14)
N2–Co–N4	166.28(13)
N2–Co–N5	92.86(13)
N2–Co–N6	88.43(13)
N3–Co–N4	82.46(14)
N3–Co–N5	88.69(13)
N3–Co–N6	92.08(13)
N4–Co–N5	89.59(13)
N4–Co–N6	89.32(13)
N5–Co–N6	178.57(13)

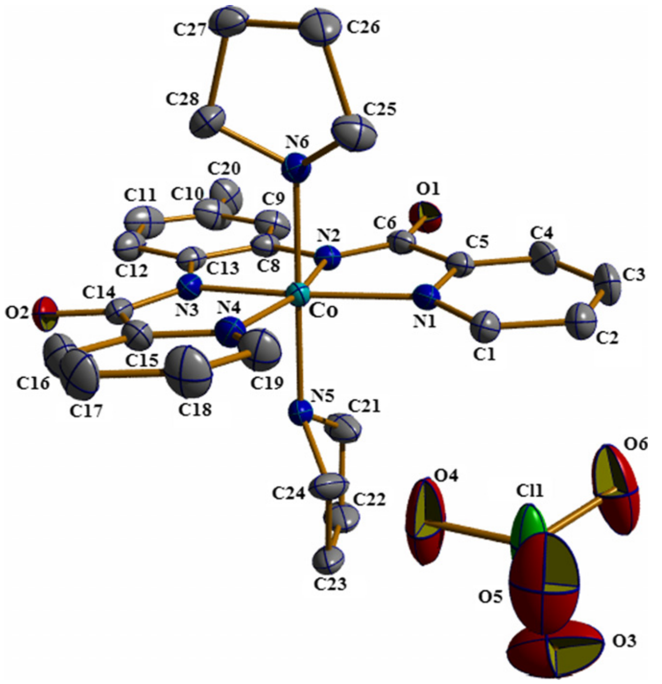

Fig. 1. The asymmetric unit of complex **1a** with the atom labeling scheme. Displacement ellipsoids are drawn at the 50% probability level; H atoms are omitted for clarity.

Of the four Co–N bonds in the equatorial plane, the $Co–N_{amide}$ bond distances [Co–N2 = 1.892(3) Å and Co–N3 = 1.892(3) Å], which are comparable to the $Co–N_{amide}$ values [1.885(2) Å and 1.891(1) Å] in *trans*-$[Co^{III}(bpb)(prldn)_2]NCS$, are indicative of strong bonding between the deprotonated amide nitrogens and the cobalt center. This is in agreement with the fact that the deprotonated amide nitrogen is a very strong σ-donor. The deprotonated mode of coordination of the amide nitrogen atoms is also evident from the absence of the amide proton signals in the ^1H NMR spectrum of complex **1a** (*vide infra*). The bond distances to the pyridine nitrogen atoms [Co–N1 = 1.997(3) Å and Co–N4 = 1.994(3) Å] are longer than those to N2 and N3, which is in accord with the lower donor ability of the pyridine nitrogen atoms. The N–Co–N bond angles in the equatorial plane consist of one which is larger than 90° [N1–Co–N4 = 110.63(13)°] and three smaller bite angles [N1–Co–N2 = 82.88(13)°, N2–Co–N3 = 84.10(14)°, and N3–Co–N4 = 82.46(14)°]. This indicates that there might be some strain in the coordination due to the rigid geometry of the ligand. The dihedral angle between the two pyridyl rings of the ligand is 15.0°. The dihedral angles between the central benzene plane and the two pyridyl rings are 10.7° and 5.5°. This observation can be attributed to the close intramolecular contact that occurs between the two H atoms in the 6-positions of the pyridyl rings; the H1···H18 distance of 2.05 Å is significantly less than the sum of the van der Waals radii (2.40 Å). The effect would be expected to be more pronounced if the ligand were perfectly planar [38]. The C–O, $C_{pyridyne}$–N, and $C_{carboxy}$–N bond distances agree well with those reported for related complexes [16,20,39–41].

All *cis* N_{eq}–Co–N_{ax} bond angles are within 3° of the ideal right-angle. The *trans*-axial N5–Co–N6 unit with a bond angle of 178.57(13)° is essentially linear. The distances between the cobalt atom and the two axial nitrogen donor atoms differ only slightly [Co–N5 = 1.992(3) Å and Co–N6 = 2.012(3) Å] and compare well with the Co–N distances found in *trans*-$[Co^{III}(bpb)(prldn)_2]NCS$ [25].

A further interesting feature of the structure of **1a** is the intermolecular hydrogen bonding (Table 3). The structure consists of chains of cations linked by rather strong N–H···O=C hydrogen bonds zig-zagging along the *c* axis (Fig. 2); the anions are not involved in hydrogen bonding.

Table 3
Hydrogen bond lengths (Å) and angles (°) for (**1a**)

D–H···A	D–H (Å)	H···A (Å)	D···A (Å)	D–H···A (°)
N5–H5···O2A	0.83(5)	2.06(5)	2.847(4)	159(4)
N6–H6···O1B	0.87(5)	2.07(5)	2.896(4)	158(4)

Symmetry operations for equivalent atoms: (A) $1-x$, $1-y$, $1-z$ and (B) $1-x$, $1-y$, $-z$.

3.3. Spectroscopic studies

The octahedral geometry of complex **1a** is evident from the X-ray structure analysis (Fig. 1). An octahedral *trans* structure for other complexes (**2a**–**4a**, **1b**–**4b**) can be inferred based on the similarity of the spectroscopic data of these complexes with those of complex **1a**. The FT-IR data of the complexes are listed in Section 2. Meaningful information regarding the bonding sites of the ligand molecules can be obtained by comparing the IR spectra of the cobalt complexes with those of the uncomplexed ligands. In the IR spectra of H_2Mebpb and H_2cbpb a band characteristic of the NH group is observed in the 3295–3305 cm^{-1} region. The disappearance of this band in the IR spectra of the complexes confirms that the ligands coordinate in their deprotonated form [17]. The bands corresponding to the amine N–H stretching vibrations are shifted to lower frequencies by about 98–265 cm^{-1} relative to the uncoordinated amines, which is in accord with expectation. Two sharp C=O stretching vibration bands at 1689 and 1659 cm^{-1} for H_2Mebpb and 1661 and 1697 cm^{-1} for H_2cbpb are shifted to lower frequencies upon coordination of the deprotonated amide, which is in agreement with the data reported for related complexes [31]. The C–N stretching vibration of medium intensity appearing at 1520 cm^{-1} for H_2Mebpb and at 1506 cm^{-1} for H_2cbpb undergoes a significant shift to higher frequencies in the corresponding complexes. This displacement is to be expected because of the resonance enhancement in the deprotonated amide which in turn leads to strengthening of the C–N bond [17]. The stretching vibrations due to the perchlorate and hexafluorophosphate anions appear in the 1080–1120 cm^{-1} and 840–846 cm^{-1} regions, respectively [42].

The UV–Vis data are presented in the Experimental section. The electronic spectra of the *trans*-$[Co^{III}(Mebpb)(amine)_2]ClO_4$ complexes (**1a**–**4a**) consist of ligand field transitions with low intensity ($180 < \varepsilon < 235$) which, depending on the axial amine ligand field strength, appear in the 610–689 nm region, and intense LMCT

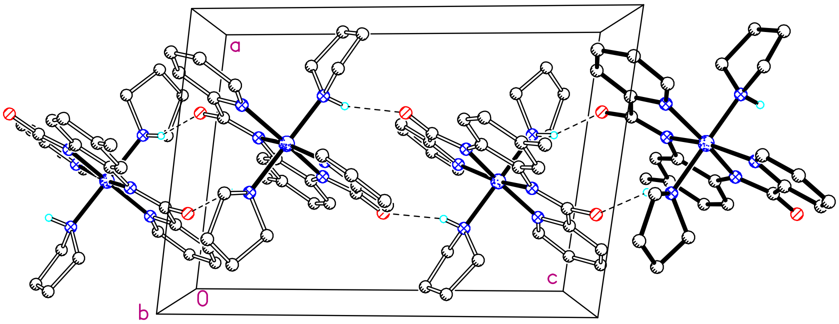

Fig. 2. A view, along the *b* axis, of the packing of **1a**. Hydrogen bonding is shown as dashed lines. Anions have been omitted, together with H atoms not involved in the hydrogen bonding.

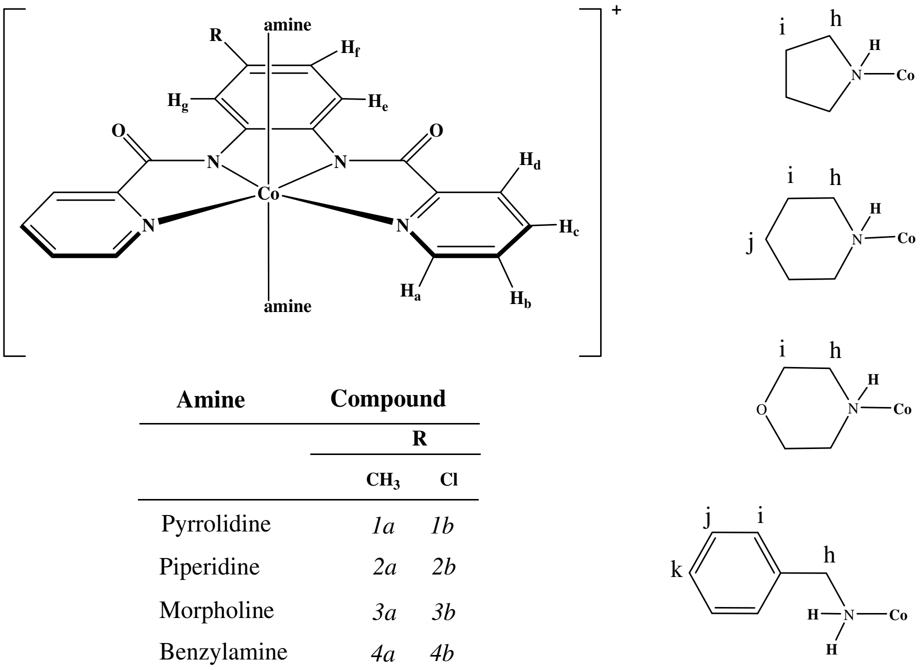

Amine	Compound	
	R	
	CH_3	Cl
Pyrrolidine	*1a*	*1b*
Piperidine	*2a*	*2b*
Morpholine	*3a*	*3b*
Benzylamine	*4a*	*4b*

Scheme 2.

transitions appearing in the 412–418 nm region. Similar transitions have been observed in the electronic absorption spectra of *trans*-$[Co^{III}(cbpb)(amine)_2]X$ complexes (**1b**–**4b**) with a blue shift of about 3–25 nm in the position of all the absorption bands relative to those of *trans*-$[Co^{III}(Mebpb)(amine)_2]ClO_4$ complexes (d–d transitions, 607–656 nm and CT transitions, 405–410 nm).

The ^1H NMR spectroscopic measurements were performed on samples in CD_3CN and $CDCl_3$ solutions. Scheme 2 displays the labeling system. The assignments are based on comparisons with corresponding rhodium(III), iridium(III), organocobalt(III) and ruthenium(II) complexes and by integrated area ratios [17,18,43–45].

The absence of the amido N–H resonance in the spectra of the complexes indicates that the ligand is coordinated to cobalt in its deprotonated form. The proton signals of the equatorial amide ligand in the complexes are generally shifted downfield relative to the free ligand. As expected, the most significant downfield shifts correspond to the protons *ortho* to the pyridyl nitrogen, H_a, and *ortho* to the nitrogen substituent on the diamido benzene group, $H_{e,g}$ [44]. The broad doublet of doublet at *ca.* $\delta = 9.39–9.46$ is assigned to H_a.

Although the chemical shifts of H_f were found to be virtually unaffected by the axial ligand, chemical shifts of $H_{e,g}$ and H_a of the cobalt complexes varied significantly. In general, δ ($H_{e,g}$) changes in the same direction as δ (H_a) but to a larger extent. The changes in the chemical shift of H_c and H_d are in line with the donor ability of the axial ligands and the UV–Vis spectral data. The trend observed in δ (H_c, H_d) for complexes **1a**–**4a**, bzlan > prldn > pprdn > mrpln, conforms to the σ-donating strength of the axial ligands, which in turn is evident from the electrochemistry of these complexes.

The appearance of the signals due to the amine protons indicates the coordination of two amine ligands in the axial positions. Aside from the aromatic protons of benzylamine which appear at about 6.74–7.12 ppm, other proton resonances of the axial amines appear between about 0.91 and 3.55 ppm.

The ^1H NMR spectra of *trans*-$[Co^{III}(cbpb)(amine)_2]^+$ complexes (**1b**–**4b**) show features similar to those observed for *trans*-$[Co^{III}(Mebpb)(amine)_2]^+$ complexes. As expected, the protons on the benzene ring exhibit slight downfield shifts in the peak positions in the $[Co^{III}(cbpb)(amine)_2]^+$ complexes, demonstrating the electron-withdrawing effect of chloro substitution in the equatorial $cbpb^{2-}$ ligand.

3.4. Electrochemistry

Cyclic voltammograms of the ligands and complexes in acetonitrile solutions with 0.1 M $[N(n\text{-}Bu)_4]PF_6$ as the supporting electrolyte were recorded at a glassy carbon working electrode. The approximate concentrations of the compounds were 1×10^{-3}–10^{-6} M.

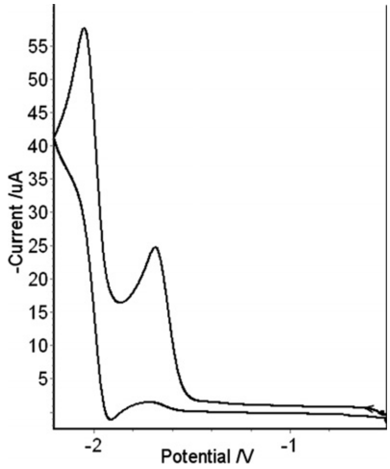

Fig. 3. Cyclic voltammogram of H_2Mebpb ligand in acetonitrile solution at 298 K. Scan rate: 100 mV s^{-1}, $c = 2.8 \times 10^{-3}$ M.

3.4.1. Electrochemistry of the ligands

The cyclic voltammograms of the ligands and their complexes were conducted at 25 °C under an argon atmosphere. It is evident from the cyclic voltammogram of H_2Mebpb, displayed in Fig. 3, that the ligand is electroactive over a range from −0.5 to −2.2 V. Two ligand-centered reductions are observed at −1.89 V and −2.2 V (Fig. 3). These reductions are attributed to the pyridyl rings and are shifted to more positive values in the corresponding complexes (Table 4). The tendency of the ligand towards reduction is apparently increased due to the transfer of electron density to the metal center [46].

The cyclic voltammogram of H_2cbpb shows features similar to those observed for H_2bpb, with an anodic shift in the peak positions resulting from the electron-withdrawing nature of the chloro substitution in the H_2cbpb ligand.

3.4.2. Electrochemistry of the complexes in the absence of amines

The reduction potentials for the cobalt complexes are summarized in Table 4. The cyclic voltammogram of the representative complex, *trans*-$[Co^{III}(Mebpb)(pprdn)_2]ClO_4$ (**2a**), is shown in Fig. 4a. An interesting observation in the cyclic voltammetric measurements of these cobalt(III) complexes is the presence of a nearly reversible oxidative response in the range of $E_{1/2} = 0.98–1.01$ V (Fig. 4, Table 4) (the first oxidation process, which can be assigned as mainly ligand-centered, occurs at virtually identical potentials).

The next reduction peak observed over the range of −0.31 to −0.53 V in (**1a**–**4a)** complexes, and −0.22 to −0.49 V in (**1b**–**4b)** complexes, is metal-centered. This is supported by the relative sensitivity of Co^{III}/Co^{II} reduction potentials to the nature of the axial amine ligand. From the E_{pc1} values (Table 4), it is evident that

Table 4
Redox potentials of (**1a**–**4a**) and (**1b**–**4b**) cobalt complexes in acetonitrile[a]

No.	Compound	$E_{1/2}$[b]	Epc1	Epa1	Epc2	Epa2	Epc3	Epa3	Epc4	Epa4
1a	$[Co(Mebpb)(Prldn)_2]ClO_4$	1.01	−0.53	−0.14		−1.28	−1.42		−2.08	−2.0
2a	$[Co(Mebpb)(Pprdn)_2]ClO_4$	1.03	−0.42	−0.01		−1.24	−1.39		−2.06	−1.99
3a	$[Co(Mebpb)(Mrpln)_2]ClO_4$	1.04	−0.31	0.03		−1.23	−1.40		−2.09	−2.01
4a	$[Co(Mebpb)(Bzlan)_2]ClO_4$	0.98	−.049	−0.05		−1.26	−1.38		−2.05	−1.97
1b	$[Co(cbpb)(Prldn)_2]PF_6$	1.16	−0.48	−0.13	−1.28	−1.19	−1.41	−1.32	−2.00	−1.92
2b	$[Co(cbpb)(Pprdn)_2]PF_6$	1.16	−0.35	−0.06	−1.23	−1.17	−1.38	−1.32	−2.00	−1.92
3b	$[Co(cbpb)(Mrpln)_2]ClO_4$	1.19	−0.22	0.33	−1.24	−1.15	−1.35	−1.31	−2.00	−1.93
4b	$[Co(cbpb)(Bzlan)_2]PF_6$	1.12	−0.49	−0.002	−1.25	−1.13	−1.43	−1.32	−2.01	−1.92

[a] Potentials are vs. $Fc^{+/0}$ in 0.1 M TBAH, $T = 293$ K. Scan rate 100 mV/s. Approximate concentrations: 1×10^{-3}–10^{-6} M.

[b] $E_{1/2} = 0.5(E_c + E_a)$.

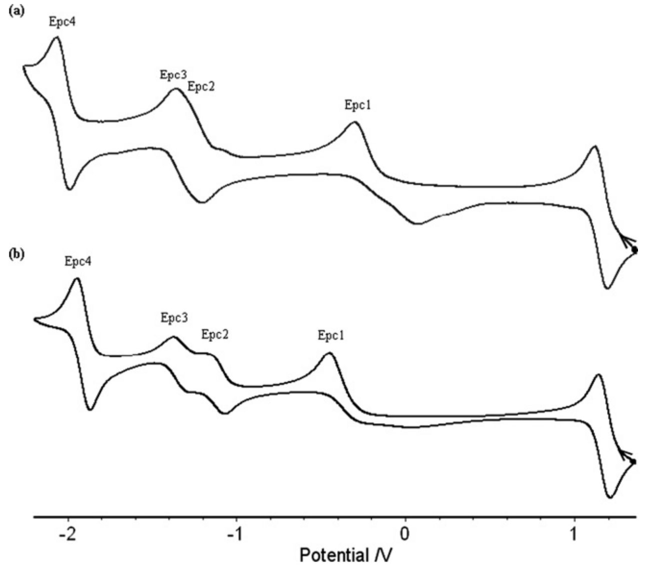

Fig. 4. Cyclic voltammograms of $[Co^{III}(Mebpb)(pprdn)_2]ClO_4$, $c = 1.8 \times 10^{-3}$ M (a), and $[Co^{III}(cbpb)(bzlan)_2]PF_6$, $c = 1.2 \times 10^{-3}$ M (b), in acetonitrile at 298 K. Scan rate, 100 mV s^{-1}.

stronger axial ligands shift the reduction potentials to more negative values. In general the Co^{III}/Co^{II} reductions for all these complexes are electrochemically irreversible in nature [19]. Accordingly, we assume that the lack of reversibility observed (Fig. 4) is most likely due to the loss of axial ligands from the cobalt(II) complex, because the electron is added to the antibonding d_{z^2} orbital [47].

$$[Co^{III}(Mebpb)(amine)_2]^+ + e^- \overset{MeCN}{\rightarrow} [Co^{II}(Mebpb)] + 2\ amine \qquad (1)$$

Owing to the very facile substitution of the axial ligands in the reduced form of these cobalt(III) complexes, electrochemical reversibility for the Co^{III}/Co^{II} couple is not observed. The oxidation of $[Co^{II}(Mebpb)(MeCN)]$ adduct occurs at much higher potentials.

The Co^{III}/Co^{II} cathodic wave in all $[Co^{III}(Mebpb)(amine)_2]^+$ complexes is followed by two overlapping redox waves, resulting from the combination of the Co^{II}/Co^{I} couple [48] and the redox couple corresponding to one of the pyridyl rings (Fig. 4a). In the $[Co^{III}(cbpb)(amine)_2]^+$ complexes, however, these couples are resolved (Fig. 4b). The final electrochemically reversible reduction couple observed in the voltammograms is related to the second pyridyl ring, that appears between $E_{1/2} = -2.01$ and -2.05 V for $[Co^{III}(Mebpb)(amine)_2]^+$ and at $E_{1/2} = -1.96$ V for $[Co^{III}(cbpb)(amine)_2]^+$ complexes. Additional evidence produced in substantiation of this fact are the results obtained from the cyclic voltammetric studies of the Ni(Mebpb) complex, that shows only two reduction waves in the range −1.57 to −2.04 V, attributed to the consecutive reduction of the two pyridyl rings [49]. Similar results have been reported for Ni(bpb) and Ni(bpen) complexes by Fenton et al. [46].

The σ-donor strength of the axial ligands also has a significant influence on the Co^{III}/Co^{II} reduction process, and the tendency of Co^{III} towards reduction increases as the axial ligand becomes a weaker donor. These observations are compatible with the ^{H} NMR and UV–Vis spectroscopic data.

A similar behavior has been found for $[Co^{III}(cbpb)(amine)_2]^+$ complexes. Fig. 4b shows the cyclic voltammogram of $[Co^{III}(cbpb)(bzlan)_2]PF_6$ (**4b**) as an example. In general the redox couples of $[Co^{III}(cbpb)(amine)_2]^+$ complexes are shifted to more positive values relative to those of the corresponding $[Co^{III}(Mebpb)(amine)_2]^+$ complexes, demonstrating the electron-withdrawing effect of chloro substitution on the electron density of the system. Similar results have been reported by Che et al. [16,43] and Ray and Mukherjee [19].

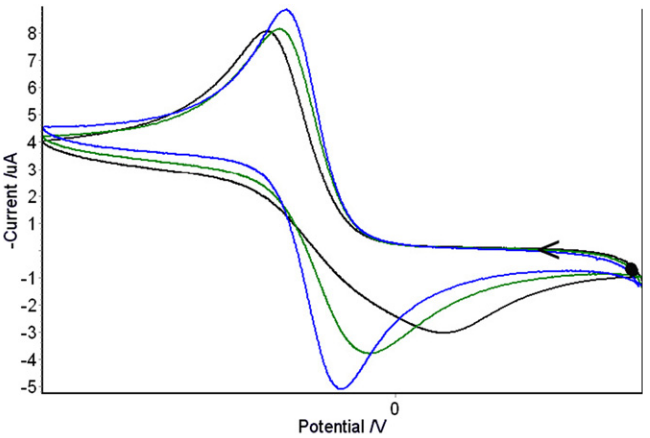

Fig. 5. Cyclic voltammograms of $[Co^{III}(Mebpb)(pprdn)_2]ClO_4$, **2a**, at different piperidine concentrations ratios (0, — black), (50, — green), (100,— blue) in acetonitrile containing 0.1 M TBAH as supporting electrolyte at 298 K. Scan rate 100 mV s^{-1}, $c = 1.5 \times 10^{-3}$ M. (For interpretation of the references to colour in this figure legend, the reader is referred to the web version of this article.)

3.4.3. Electrochemistry of the complexes in the presence of amines. It is well established that in many *trans*-$[Co^{III}(N_2O_2)(L)_2]^+$ Schiff base complexes, the first irreversible reduction process (Co^{III}/Co^{II}) can become quasi-reversible under controlled concentration conditions [47,50]. In an attempt to examine the possibility of reversible electrochemical behavior in analogous amido complexes, the electrochemistry of $[Co^{III}(Mebpb)(pprdn)_2]ClO_4$ was carried out in the presence of excess amine. In the absence of additional amine the first reduction processes of (Co^{III}/Co^{II}) is electrochemically irreversible ($\Delta E = 410$ mV). Upon addition of excess amine, the oxidation wave of Co(II) is shifted towards more negative potentials (Fig. 5) ($\Delta E = 107$ mV), indicating the increased formation of six-coordinated adducts; i.e. the electrode process is preceded by a reversible chemical reaction

$$[Co^{II}(Mebpb)] + excess\ amine[Co^{III}(Mebpb)(amine)_2]^+ + e^- \qquad (2)$$

The redox potential of the Co(II/I) couple is not significantly changed by the addition of excess amine and can be regarded as approximately independent.

4. Conclusion

The combination of spectroscopic, crystallographic, and electrochemical measurements we have described has illustrated the main features of the coordination and redox chemistry of the *trans*-$[Co^{III}(Mebpb)(amine)_2]ClO_4$ and *trans*-$[Co^{III}(cbpb)(amine)_2]PF_6$ complexes. The coordination geometry around the Co^{III} center in these complexes is distorted octahedral. Electrochemical studies reveal that the first reduction process Co^{III}/Co^{II} is irreversible and strongly influenced by the nature of the axial amines. When the axial ligands are changed from morpholine to pyrrolidine a change in the Co^{III}/Co^{II} cathodic peak of 220 mV for Mebpb complexes and 260 mV for cbpb complexes is observed. This process becomes quasi-reversible upon the addition of excess amine. The two redox waves, resulting from the combination of the Co^{II}/Co^{I} couple and the redox couple corresponding to one of the pyridyl rings, overlap in $[Co(Mebpb)(amine)_2]^+$, but are resolved in $[Co(cbpb)(amine)_2]^+$ complexes. In general, the redox couples of $[Co(cbpb)(amine)_2]^+$ complexes are shifted to more positive values relative to those of the corresponding $[Co(Mebpb)(amine)_2]^+$ complexes due to the electron-withdrawing effect of chloro substitution.

Acknowledgement

Partial support of this work by the Isfahan University of Technology Research Council is gratefully acknowledged.

Appendix A. Supplementary data

CCDC 681508 contains the supplementary crystallographic data for **1a**. These data can be obtained free of charge via http://www.ccdc.cam.ac.uk/conts/retrieving.html, or from the Cambridge Crystallographic Data Centre, 12 Union Road, Cambridge CB2 1EZ, UK; fax: (+44) 1223-336-033, or e-mail: deposit@ccdc.cam.ac.uk. Supplementary data associated with this article can be found, in the online version, at doi:10.1016/j.poly.2008.05.031.

References

[1] C. Jubert, A. Mohamadou, C. Gerard, S. Brandes, A. Tabard, J.P. Barbier, Inorg. Chem. Commun. 6 (2003) 900.

[2] J. Lin, J.Y. Zhang, Y. Xu, X.K. Ke, Z. Guo, Acta Crystallogr., Sect. C 57 (2001) 192.

[3] D.A. Conlon, N. Yasuda, Adv. Synth. Catal. 343 (2001) 137.

[4] H. Kurosaki, R.K. Sharma, S. Aoki, T. Inoue, Y. Okamoto, Y. Sugiura, M. Doi, T. Ishida, M. Otsuka, M. Goto, J. Chem. Soc., Dalton Trans. (2001) 441.

[5] J. Zhang, Q. Liu, C. Duan, Y. Shao, J. Ding, Z. Miao, X.-Z. You, Z. Guo, J. Chem. Soc., Dalton Trans. (2002) 591.

[6] W.-H. Leung, J.-X. Ma, V.W.-W. Yam, C.-M. Che, C.-K. Poon, J. Chem. Soc., Dalton Trans. (1991) 1071.

[7] B.M. Trost, I. Hachiya, J. Am. Chem. Soc. 120 (1998) 1104.

[8] S.R. Collinson, T. Gelbrich, M.B. Hursthouse, J.H.R. Tucker, Chem. Commun. (2001) 555.

[9] I. Huc, M.J. Krische, D.P. Funeriu, J.-M. Lehn, Eur. J. Inorg.Chem. (1999) 1415.

[10] J.D. Epperson, L.-J. Ming, G.R. Baker, G.R. Newkome, J. Am. Chem. Soc. 123 (2001) 8583.

[11] U. Beckmann, E. Bill, T. Weyhermuller, K. Wieghardt, Inorg. Chem. 42 (2003) 1045.

[12] M. Ray, D. Ghosh, Z. Shirin, R. Mukherjee, Inorg. Chem. 36 (1997) 3568.

[13] C.-M. Che, W.-H. Leung, C.-K. Li, H.-Y. Cheng, S.M. Peng, Inorg. Chim. Acta 196 (1992) 43.

[14] M. Ray, S. Mukerjee, R.J. Mukherjee, Chem. Soc. Dalton Trans. (1990) 3635.

[15] A.K. Patra, R. Mukherjee, Inorg. Chem. 38 (1999) 1388.

[16] S.-T. Mak, W.-T. Wong, V.W.-W. Yam, T.-F. Lai, C.-M. Che, J. Chem. Soc., Dalton Trans. (1991) 1915.

[17] R.L. Chapman, R.S. Vagg, Inorg. Chim. Acta 33 (1979) 227.

[18] D.J. Barnes, R.L. Chapman, R.S. Vagg, E.C. Walton, J. Chem. Eng. Data 23 (1978) 349.

[19] M. Ray, R.N. Mukherjee, Polyhedron 11 (1992) 2929.

[20] M. Ray, R. Mukherjee, J.F. Richardson, R.M. Buchanan, J. Chem. Soc., Dalton Trans. (1993) 2451.

[21] A. Hori, T. Ozawa, H. Yoshida, Y. Imod, Y. Kufibayashi, E. Nakano, N. Azuma, Inorg. Chim. Acta 281 (1998) 207.

[22] S.K. Dutta, U. Beckmann, E. Bill, T. Weyhermuller, K. Wieghardt, Inorg. Chem. 39 (2000) 3355.

[23] A.K. Patra, M. Ray, R. Mukherjee, Inorg. Chem. 39 (2000) 652.

[24] J.M. Rowland, M.L. Thornton, M.M. Olmstead, P.K. Mascharak, Inorg. Chem. 40 (2001) 1069.

[25] M. Amirnasr, K.J. Schenk, S. Meghdadi, Inorg. Chim. Acta 338 (2002) 19.

[26] S.L. Jain, P. Bhattacharyya, H.L. Milton, A.M.Z. Slawin, J.A. Crayston, J.D. Woollins, J. Chem. Soc., Dalton Trans. (2004) 862.

[27] O. Belda, C. Moberg, Coord. Chem. Rev. 249 (2005) 727.

[28] J. Singh, G. Hundal, R. Gupta, Eur. J. Inorg. Chem. (2008) 2052.

[29] Z.N. Zahran, D.R. Powell, G.B. Richter-Addo, Inorg. Chim. Acta 359 (2006) 3084.

[30] S. Meghdadi, H.R. Khavasi, S. Nalchigar, Acta Crystallogr., Sect. E 62 (2006) o5492.

[31] S. Meghdadi, M. Amirnasr, V. Langer, A. Zamanpoor, Can. J. Chem. 84 (2006) 971.

[32] N.G. Connelly, W.E. Geiger, Chem. Rev. 96 (1996) 877.

[33] Nonius, COLLECT, Nonius BV, Delft, The Netherlands, 1998.

[34] A.J.M. Duisenberg, L.M.J. Kroon-Batenburg, A.M.M. Schreurs, J. Appl. Crystallogr. 36 (2003) 220.

[35] G.M. Sheldrick, SADABS, Göttingen University, Germany, 2006.

[36] A. Altomare, M.C. Burla, M. Camalli, G.L. Cascarano, C. Giacovazzo, A. Guagliardi, A.G.G. Moliterni, G. Polidori, R. Spagna, J. Appl. Crystallogr. 32 (1999) 115.

[37] G.M. Sheldrick, SHELXTL Version 6, Bruker AXS Inc., Madison, WI, USA, 2001.

[38] W.-T. Wong, C.-M. CHE, Acta Crystallogr., Sect. C 50 (1994) 1407.

[39] N. Azuma, T. Ozawa, S. Tsuboyama, J.Chem. Soc., Dalton Trans. (1994) 2609.

[40] A.K. Patra, R. Mukherjee, Polyhedron 18 (1999) 1317.

[41] Y. Yang, F. Diederich, J.S. Valentine, J. Am. Chem. Soc. 113 (1991) 7195.

[42] K. Nakamoto, Infrared and Raman Spectra of Inorganic and Coordination Compounds Part II: Application in Coordination, Organometallic and Bioinorganic Chemistry, 5th ed., Wiley Interscience, New York, 1997.

[43] S.-T. Mak, V.W.-W. Yam, C.-M. Che, J. Chem. Soc., Dalton Trans. (1990) 2555.

[44] C.F. Fortney, R.E. Shepherd, Inorg. Chem. Commun. 7 (2004) 1065.

[45] C.F. Fortney, S.J. Geib, F.-T. Lin, R.E. Shepherd, Inorg. Chim. Acta 358 (2005) 2921.

[46] C.L. Weeks, P. Turner, R.R. Fenton, P.A. Lay, J. Chem. Soc., Dalton Trans. (2002) 931.

[47] A. Bottcher, T. Takeuchi, K.I. Hardcastle, T.J. Meade, H.B. Gray, D. Cwikel, M. Kapon, Z. Dori, Inorg. Chem. 36 (1997) 2498.

[48] A.K. Patra, M. Ray, R. Mukherjee, J. Chem. Soc., Dalton Trans. (1999) 2461.

[49] A. Amiri, M. Amirnasr, S. Meghdadi, K. Mereiter, V. Ghodsi, A. Gholami, submitted for publication.

[50] M. Amirnasr, R. Vafazadeh, A. Mahmoudkhani, Can. J. Chem. 80 (2002) 1196.